Tr. J. of Physics
23 (1999) , 701 – 707.

Semiconductor and Dielectric Microcavity Spectroscopy

Ali SERPENGÜZEL
Department of Physics, Bilkent University
Bilkent, 06533 Ankara-TURKEY

Received 01.03.1999

Abstract

Semiconductor and dielectric microcavities are used for the localization of photons as well as the enhancement of photon density of states. The enhancement of photoluminescence, electroluminescence, and lasing by the use of microcavities leads to novel active and passive optoelectronic and photonic devices such as channel droppping filters, semiconductor lasers, and resonant cavity enhanced devices. Experimental results showing photoluminescence enhancement in active planar, lasing in active ellipsoidal microcavities as well as light scattering in passive and spherical microcavities are presented.

1. Introduction

Due to their unique optical properties, microcavities (μ-cavities) continue to receive attention [1]. In a μ-cavity, two electromagnetic and quantum electrodynamic effects occur. First, the μ-cavity acts as a resonator for light rays with specific wavelengths, which correspond to the μ-cavity modes. Second, in a μ-cavity, the photon density of states (DOS) is enhanced at the cavity modes, when compared with the continuum of photon states of the bulk. The spontaneous emission (SE) cross-sections at the resonances are larger than the bulk SE cross-sections because of the enhanced photon DOS [2]. Also, the SE cross-sections in between the resonances are smaller than the bulk SE cross-sections. Alteration of SE in planar microcavities has been both observed experimentally [3] and calculated theoretically [4]. These properties of μ-cavities are used in resonant cavity enhanced (RCE) photonic devices, which are wavelength selective and ideal for wavelength division multiplexing (WDM) applications, such as RCE photodiodes [5], RCE light emitting diodes [6], vertical cavity surface emitting lasers [7], μ-disk [8], and μ-wire [9] lasers.

2. Microcavity Geometries

Typical μ-cavity geometries are listed in Table 1. In all the geometries, if the optical path is equal to an integral number of wavelengths, a resonance is formed. The resonance wavelengths (λ_ℓ) satisfy the condition ($\lambda_\ell = Ln/\lambda$), where λ is the mode number, L the round trip distance, and n the refractive index. In a planar μ-cavity light is confined in the longitudinal dimension using two parallel mirrors, and there are degeneracies in the the transverse and the lateral dimensions. These degeneracies might be lifted by the transverse and the lateral dimensions of the mirrors. The planar μ-cavity modes are labeled by the longitudinal mode number (ℓ). In a circular μ-cavity, e.g., a μ-disk, light is confined in the radial and polar angular dimensions by total internal reflection (TIR) [10]. However, there is a twofold (clockwise and counterclockwise) degeneracy in the polar dimension. The μ-disk resonances are labeled by the radial mode number (n) and the polar mode number (ℓ). In a spherical μ-cavity, light is confined in the radial, polar, and azimuthal dimensions by TIR. The μ-sphere resonances are described by a set of vector-spherical harmonics [11] labeled by a radial mode number (n), a polar mode number (ℓ), and an azimuthal mode number (m), which has values $\pm\ell, \pm(\ell-1), \ldots, 0$. For a μ-sphere, the m-mode resonances for a given ℓ are spectrally ($2\ell+1$) degenerate [12]. This degeneracy is lifted in the ellipsoidal geometry. In this paper, experimental results showing photoluminescence (PL) enhancement in active planar and ellipsoidal μ-cavities as well as light scattering in a passive spherical μ-cavity are presented.

3. Photoluminescence of a Planar Microcavity

Recently, visible PL from hydrogenated amorphous nitride (a-$SiN_x : H$) has been observed [13]. The alteration of PL in an a-$SiN_x : H$ μ-cavity has also been reported [14]. For the a-$SiN_x : H$ grown without NH_3 the PL extends from the red to the near-infrared. However, for the a-$SiN_x : H$ grown with NH_3, the PL is in the blue-green. These complementary colors cover the whole visible spectrum, and make a-$SiN_x : H$ suitable for color flat panel display and WDM applications. The μ-cavity fabricated without (with) NH_3 had a Au (Al) back mirror and an a-$SiN_x : H$-air interface (Al) front mirror. The details of the fabrication are given in elsewhere [15]. Figure 1(a) and (b) depicts the PL of the a-$SiN_x : H$ μ-cavity fabricated without (with) NH_3. The PL spectrum was obtained using an Ar^+ laser at 514.5 (457.9) nm and was corrected for the responsivity of the spectrometer and the photomultiplier tube (PMT). The PL is modulated by resonances, which have linewidths of $\Delta\lambda = 25$ (20) nm and quality factors of $Q = 30$ (25). The fitted values of L=1438 (1072) nm and n = 2.1 (1.6) agree with the measured values. In both Figures 1 (a) and (b) the PL of the bulk a-$SiN_x : H$ is enhanced at, and inhibited in between, the resonances. The enhancement and inhibition of the PL is understood by the modified photon DOS of the μ-cavity. The linewidth of the PL is also narrowed with respect to the linewidth of the bulk a-$SiN_x : H$, again due to the presence of the μ-cavity. The μ-cavity enhancement and inhibition of PL in a-$SiN_x : H$ opens up a variety of possibilities for optoelectronic applications such as color flat panel displays or RCE devices.

Table 1. Several μ-cavity geometries in various dimensions (**D**)

Microcavity geometry	Microcavity Schematic	D	Quantum Number	Degeneracy
Planar (Fabry-Perot)		1	Longitudinal (l)	Lateral Transverse
Circular		2	Radial(n) Polar angle(l)	2 fold ($\pm l$)
Spherical		3	Radial (n) Polar angle (l)	($2l$+1) fold
Ellipsoidal		3	Radial (n) Polar angle (l) Azimuthal (m)	2 fold ($\pm m$)

4. Elastic Light Scattering in a Spherical Microcavity

Since they confine light in all three dimensions, μ-spheres also enjoy the attention of the optical community [16]. Although a variety of linear and nonlinear optical processes have been observed in μ-droplets, photonic devices using these properties require the use of solid μ-spheres [17]. New WDM applications such as channel dropping filters can be envisioned, if the resonances of the μ-spheres are coupled to traveling waves of optical fibers [18]. In this section, the coupling between an optical fiber coupler (OFC) and a μ-sphere is treated. The details of the experimental setup can be found elsewhere [19]. The excitation source is a tunable dye laser with $\Delta\lambda = 0.025$ nm. The scattering from the μ-sphere was collected at 90° with a microscope through a polarizer and detected with a PMT. Figure 2 (a) shows the scattering spectrum at 90° from the μ-sphere obtained through a polarizer with its polarization axis at 45° to the OFC. The intensity decrease at the longer wavelength side of both spectra is due to the dye laser gain profile. A noteworthy feature of the spectrum is that resonances with $\Delta\lambda = 0.04$ nm were observed. Keeping in mind that the dye laser has $\Delta\lambda = 0.025$ nm, the measured resonance $\Delta\lambda$ are clearly limited by convolution with the laser $\Delta\lambda$. The observed resonances appear to correspond to first ($n = 1$), second ($n = 2$), and third order ($n = 3$) resonances with theoretical Q's of approximately 10^7, 10^5 and 10^3, respectively. The experimental first order resonances are considerably broadened since the dye laser $\Delta\lambda = 0.025$ nm is wider than the theoretical first order resonance $\Delta\lambda = 2 \times 10^{-5}$ nm. The fitted value of the radius **a**=15 μm and n=1.59 aggree with their measured values. The coupling of an OFC to a μ-sphere opens up a variety of possibilities in microphotonics, one of which is the use of the μ-sphere-OFC system as a channel dropping filter.

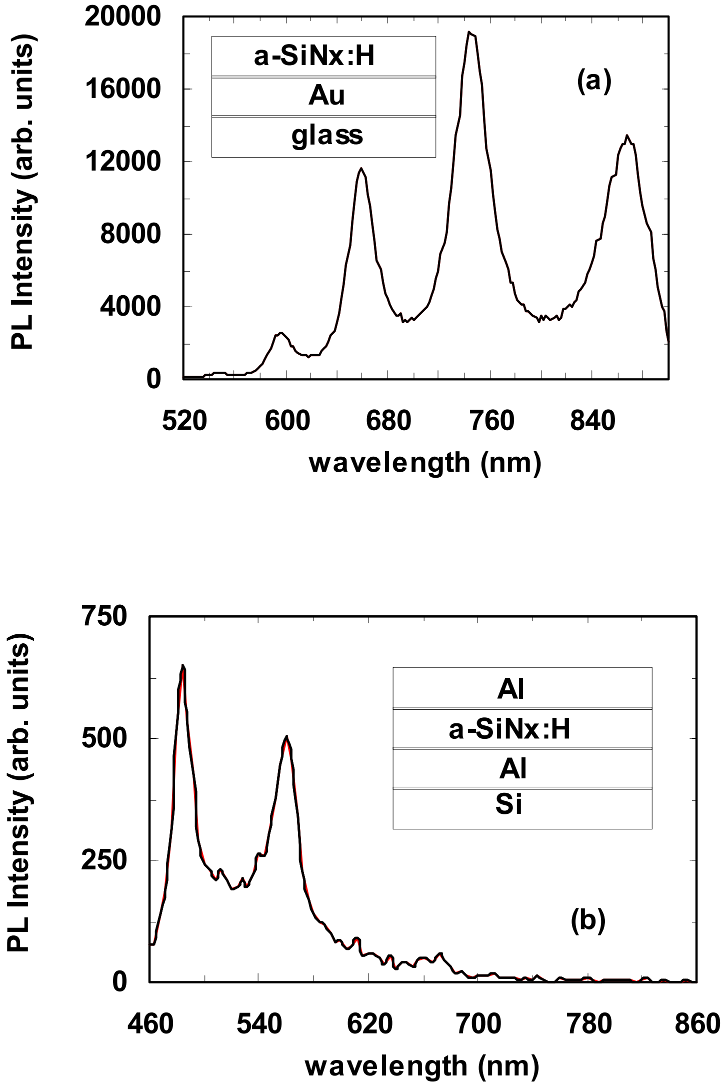

Figure 1. PL of a-$SiN_x : H\mu$-cavity fabricated (a) without NH_3 and (b) with NH_3.

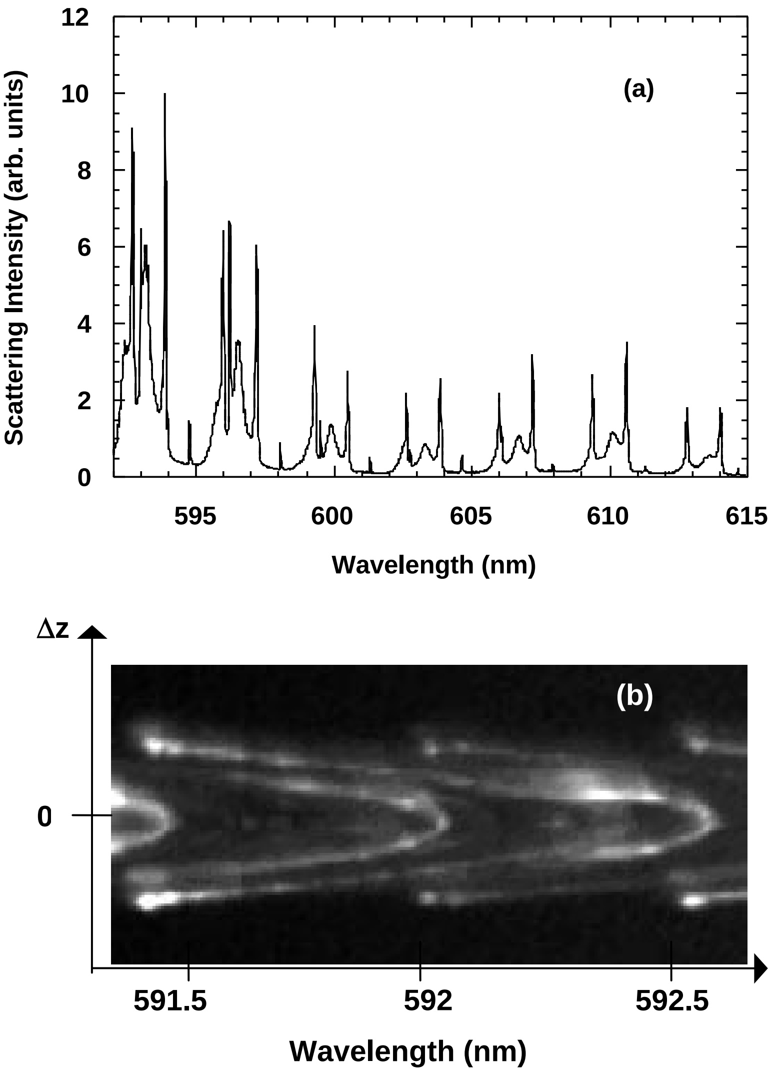

Figure 2. (a) Elastic scattering of a micropshere (b) lasing of an ellipsoidal μ-cavity.

5. Lasing in an Ellipsoidal Microcavity

Spherical μ-cavities can be deformed into ellipsoids such as oblates or prolates. For a slightly deformed μ-sphere, the frequencies of the normal azimuthal modes, are no longer degenerate but, vary with position along the μ-sphere rim. In this section, the observation of the wavelength variation of the laser emission that emerges from the entire rim of slightly deformed μ-spheres doped with laser dye, i.e., $\lambda(m)$ is measured as a function of m ranging from $m = \pm n$ to $m = 0$. By using a spectrograph and a two-dimensional charge coupled device (CCD) detector, the laser emission wavelength from all points along the μ-sphere rim is recorded simultaneously. The details of the experimental setup can be found elsewhere [20]. The dependence of $\lambda(m)$ along the spectrograph slit provides information about the μ-sphere deformation amplitude as well as determining whether the μ-sphere is an oblate or a prolate spheroid. Figure 2(b) shows the CCD image recorded for an oblate μ-sphere. The $\supset -$shaped $\lambda(\Delta z)$ curve corresponds to the lasing spectrum of all azimuthal mode number m resonances with a fixed radial mode order n and polar mode number ℓ. The cause of the $\supset$-shaped curve is attributed to the dispersion of $\lambda(m)$ of the lasing radiation that leaks from the entire μ-sphere rim, starting with the μ-sphere equator, extending to various portions of the rim, and finally ending with the μ-sphere poles. The shape of $\lambda(\Delta z)$ is parabolic with respect to Δz. From the CCD image, the ellipticity (**e**) of the oblate was determined to be **e**=-0.004.

Acknowledgments

I would like to acknowledge the partial support of this research by the Scientific and Technical Research Council of Turkey Grant TBAG-1368 and the International Center for Theoretical Physics Grant 95-500 RG/PHYS/AS.

References

[1] J. Rarity and C. Weisbuch, eds., Microcavities and Photonic Bandgaps: Physics and Applications (Kluwer, Dordrecht, 1996).

[2] E. M. Purcell, Phys. Rev. **69**, 681 (1946).

[3] F. De Martini, G. Innocenti, G. R. Jacobowitz, and P. Mataloni, Phys. Rev. Lett. **59**, 2955 (1987).

[4] H. Yokoyama, S. D. Brorson, J. Appl. Phys. **66**, 4801 (1989).

[5] M. S. Ünlü and S. Strite, J. Appl. Phys. **78**, 607 (1995).

[6] E. F. Schubert, Y.-H. Wang, A. Y. Cho, l. W. Tu, and G. J. Zydzik, Appl. Phys. Lett. **60**, 921 (1992).

[7] H. Yokoyama, K. Nishi, T. Anan, H. Yamada, S. D. Brorson, and E. P. Ippen, Appl. Phys. Lett. **57**, 2814 (1990).

[8] S. L. McCall, A. F. J. Levi, R. E. Slusher, S. J. Pearton, and R. A. Logan, Appl. Phys. Lett. **60**, 289 (1992).

[9] J. P. Zhang, D. Y. Chu, S. L. Wu, S. T. Ho, W. G. Bi, C. W. Tu, and R. C. Tiberio, Phys. Rev. Lett. **75**, 2678 (1995).

[10] S. C. Hill and R. E. Benner, in Optical Effects Associated with Small Particles, P. W. Barber and R. K. Chang, eds. (World Scientific, Singapore, 1988), pp. 3-61.

[11] C. F. Bohren and D. R. Huffman, Absorption and Scattering of Light by Small Particles, (John Wiley and Sons, New York 1983).

[12] H.-M. Lai, P. T. Leung, K. Young, P. W. Barber, and S. C. Hill, Phys. Rev. A **41**, 5187 (1990).

[13] A. Aydinli, A. Serpengüzel, D. Vardar, Solid State Commun. **98**, 273 (1996).

[14] A. Serpengüzel, A. Aydinli, and A. Bek, Optics Express **1**, 108 (1997).

[15] A. Serpengüzel, A. Aydinli, A. Bek, and M. Güre, J. Opt. Soc. Am. B. **15**, 2706, (1998).

[16] P. W. Barber and R. K. Chang, Eds., Optical Effects Associated with Small Particles, (World Scientific, Singapore, 1988)

[17] A. Serpengüzel, S. Arnold, and G. Griffel, Opt. Lett. **20**, 654 (1995).

[18] G. Griffel, S. Arnold, D. Taskent, A. Serpengüzel, J. Connolly, and N. Morris, Opt. Lett. **21**, 695 (1996).

[19] A. Serpengüzel, S. Arnold, and G. Griffel, and J. A. Lock, J. Opt. Soc. Am. B. **14**, 790 (1997).

[20] G. Chen, Md. M. Mazumder, Y. R. Chemla, A. Serpengüzel, R. K. Chang, and S. C. Hill, Opt. Lett. **18**, 1993 (1993).